

Hardware efficient seizure prediction algorithm

Sergi Consul^a, Bashir I. Morshed^a, Robert Kozma^b

^aElectrical and Computer Engineering Department, The University of Memphis, Memphis, TN, USA

^bCenter for Large-Scale Integrated Optimization and Networks (CLION), The University of Memphis, TN, USA

ABSTRACT

Epilepsy affects 2.5 million people in the USA, 15% of which cannot be treated with traditional methods. Effective treatments require reliable prediction of seizures to increase their effectiveness and quality-of-life. Phase synchronization phenomenon of two distant neuron populations for a short period of time just prior to a seizure episode is utilized for such prediction. This paper presents a hardware efficient prediction algorithm using phase-difference (PD) method instead of the commonly used phase-locking statistics (PLS). The dataset has been collected from publicly available “CHB-MIT Scalp EEG Database” that consists of scalp EEG recordings from 10 pediatric subjects with intractable seizures. The seizure channel is selected based on the maximum value of the standard deviation during seizure, while the reference channel has the minimum value of the standard deviation. Data from these two channels is conditioned with a band-pass ($f_{lc} = 10\text{Hz}$, $f_{hc} = 12.5\text{Hz}$) 6th order Chebyshev Type II filter or a FIR filter. The analytical signals are derived using Hilbert Transform to allow phase extraction. PLS and PD are calculated from the mean of the phase-differences using an overlapping sliding-window technique. PD method demonstrates the same characteristics as PLS, while achieving 2.35 times faster computation rate in MATLAB than PLS. With 51 seizure episodes, prediction latency was between 51 seconds to 188 minutes with sensitivity of 88.2%. PD yields to lower hardware requirement and reduces computational complexity.

Keywords: Epilepsy, Phase-locking statistics, Phase difference, Scalp electroencephalogram, Seizure prediction.

1. INTRODUCTION

Epilepsy, the second largest neurological disorder in the world after stroke, affects about one percent of the population in the world [1]. In the United States of America, epilepsy accounts for around 2.5 million patients [2]. Two thirds of these epileptics can be treated with drugs, and from the one third remaining, around half of them can be treated with surgery, but there are still a 15% of epileptic patients who do not respond to current methods [3]. For this 15% of patients with no current treatment, alternative techniques are being studied and rapidly emerging. One of the modalities of such treatment is Vagus Nerve Stimulation (VNS). This nerve is a paired cranial nerve that outputs sensory and motor information to and from various organs to the brain about the state of these organs. The Vagus nerve has diffused and widespread projections to the thalamus, amygdala, and forebrain and to other cortical areas. It is believed that these thalamocortical relay neurons modulate cortical excitability in such extent that influences the generation of generalized seizures [4]. Exciting VNS with implantable neuronal prosthesis via direct electrical stimulation or mechanical vibration has shown promise to reduce or eliminate seizure episodes [4].

However, continuous stimulation has been attributed to significant neuronal damage, and decreases the efficacy of the implanted prosthesis, a condition known as stimulation induced depression of neuronal excitability (SIDNE) [5]. In an effort to resolve this clinical challenge, just-in-time VNS stimulation with a closed-loop VNS system is envisioned [6-7]. Such prosthesis with the capability of seizure prediction would increase the quality of life of the non-tractable seizure patients that are stuck either with seizures or with open-loop VNS systems that have clinical side-effects, like cough, hoarseness, dyspnea, pain, paraesthesia, headaches, and voice alteration [8].

This study presents a new approach to compute the prediction of seizures, which we refer as Phase Difference (PD), which would allow the implementation of a close-loop VNS system that will be able to stimulate the Vagus Nerve only when a prediction of the seizure is made. The basis for this new prediction method is based on the work of [9] where Lachaux *et al.* measure the synchronization between two neuron populations by means of a method called Phase-

Locking Statistics (PLS). Le Van Quyen *et al.* used, for the first time, the PLS to compute the change in the dynamics in the brain activity before seizures, where it was found that PLS was able to detect this changes making it a good seizure predictor [10].

It has been shown that other predicting methods also demonstrate good performance [11,12]. In this paper, we present a hardware efficient approach with PD that yields the same performance as PLS while leading to a more efficient hardware implementation, which will lead to a smaller size and lower power consumption when implemented.

2. METHOD

This study systematically evaluates the performances of two seizure prediction algorithms by implementing the algorithms in MATLAB (MathWorks, MA, USA) to identify the hardware efficient alternative. All functions and scripts have been developed in-house except the function to load the EEG data (edfread), which uses the standard European Data Format (EDF).

2.1 The EEG Dataset

The seizure dataset has been collected from the publicly available “CHB-MIT Scalp EEG Database” [13], and consists of scalp EEG recordings from 22 pediatric subjects with intractable seizures, 5 males, ages from 3 to 22 and 17 females, ages ranging from 1.5 to 19. For each patient, there are between 9 to 42 (almost) continuous EEG recordings. In few recordings, there are jumps of 10 seconds in between recordings. Most recordings are one hour long, while some recordings are 2 or 4 hours long, or shorter if a seizure episode occurred.

The sampling rate for the recorded EEG signals is 256 samples per second with 16-bit resolution. The montage used is the International 10-20 system bipolar montage. In each recording where seizures are present, the seizure start-time and end-time are marked in a separate file by an epileptologist.

For this study, seizure data from the first 10 patients of the dataset are used (Chb01 to Chb10 - surrogate names for the actual patient’s names). Figure 1 shows a representative raw EEG data from patient 1 (ID: Chb01, Record: 03). The seizure prediction algorithm requires simultaneous data from two distinct channels, which we refer as active and reference channels. Active channel is selected based on the maximum value of the standard deviation during seizure, while the reference channel has the minimum value of the standard deviation [14].

In Table 1, a summary of the active and reference channels as well as the number of seizure recordings per patient is shown. These channels are the ones used for all the recordings of each patient. If for one patient, there is more than one active, or reference channel, the one that appear more times is the one that is used.

Table 1. Identified active and reference channels by analyzing the standard deviations of all channels for each patient, and the corresponding number of seizure episode recordings in the dataset

Patient ID	Chb01	Chb02	Chb03	Chb04	Chb05	Chb06	Chb07	Chb08	Chb09	Chb10
Active channel	FT9-FT1	C3-P3	FP1-F3	FT9-FT1	F3-C3	F3-C3	FZ-CZ	P4-O2	P4-O2	T7-P7
Reference channel	T7-FT9	FT10-T8	P4-O2	FZ-CZ	FT10-T8	FP2-F8	T7-FT9	FT10-T8	FT10-T8	FT10-T8
Number of Seizure Recordings	7	3	7	4	5	10	3	5	4	7

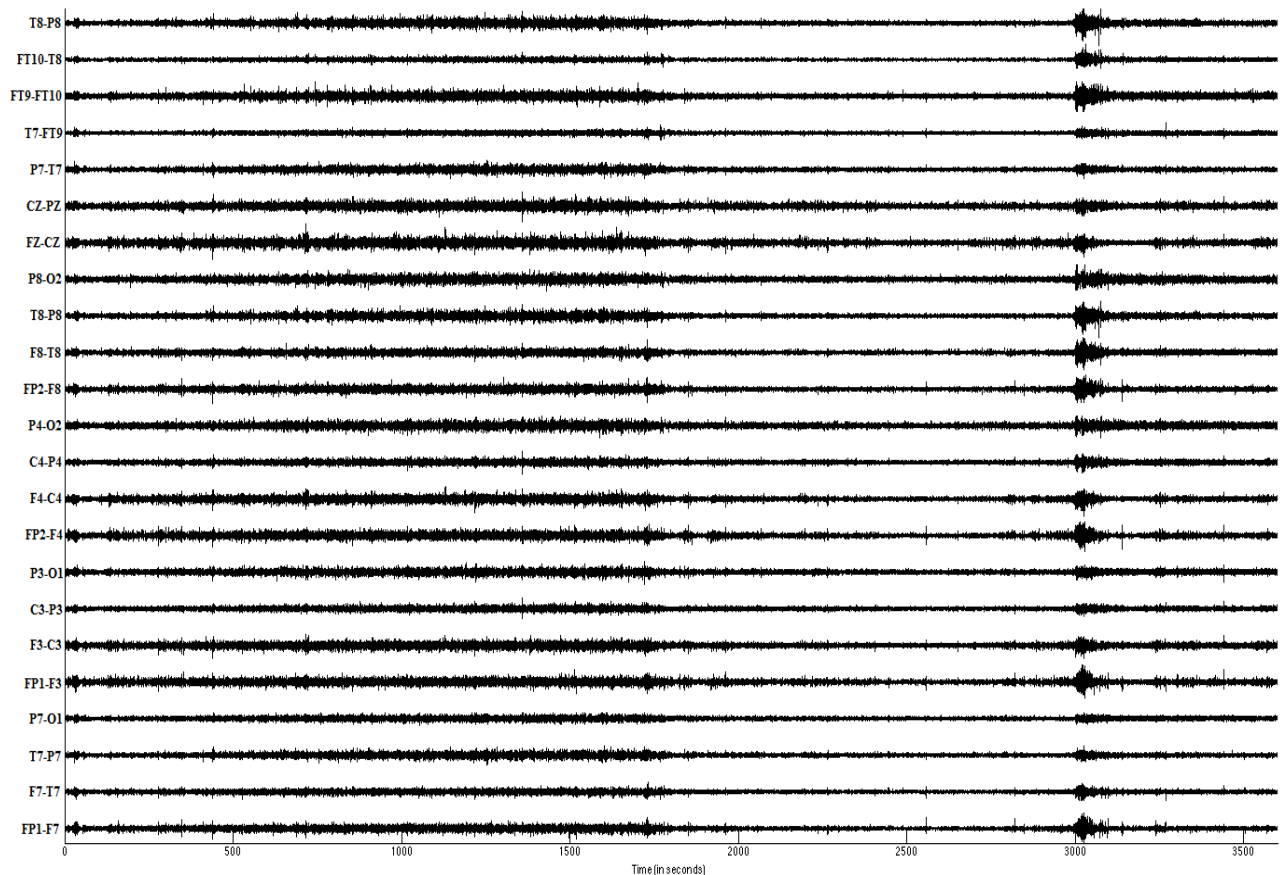


Figure 1. Temporal plot of a representative recording of raw EEG data from all channels for a patient with a seizure episode (patient ID: chb01, Record: 03).

2.2 Pre-Processing

Once the active and reference channels are identified by analyzing the standard deviations, there are certain pre-processing steps that need to be conducted before applying the seizure prediction algorithm. The pre-processing steps are to filter the raw EEG data from the two channels (active and reference), and then to compute the phase of each channel, since this analytic is needed by the two prediction algorithms studied in this work.

2.2.1 Filtering of raw EEG data

The first step of the pre-processing is to filter the raw EEG data using a digital filter. In this study, two different kinds of filters have been evaluated; a 200th order Parks-McClellan optimal finite impulse response (FIR) band-pass filter (BPF) [7], and a 6th order Chebyshev Type II infinite impulse response (IIR) BPF filter. The same cut-off frequencies ($f_{lc} = 10\text{Hz}$ and $f_{hc} = 12.5\text{Hz}$) for both filters are selected for comparative evaluation. The filter band-pass should be as narrow as possible, ideally 0 Hz bandwidth, since we need to compute the phase between channels. For practical implementation, we adhere to the technique applied previously [15] where the bandwidth (BW) is chosen to be 2.5 Hz as in this study.

For both filters, the stop-band is at least 100 dB attenuated for frequencies lower than 2.5 Hz and higher than 20 Hz. The comparative study of filters allow us to identify any performance variation in terms of seizure predication latency and accuracy by implementing the low-order hardware-efficient IIR filter in place of the higher-order FIR filter which is commonly used in the literature [16].

2.2.2 Analytical Signal and Phase calculation

For computing the seizure prediction algorithm, the phases of the active and reference channels are needed. Hence, we need to extract the phase information from the filtered EEG data by computing the Analytical Signals for each channel. This can be done by a number of methods; two of them are the use of a complex Gabor Wavelet and the use of the Hilbert Transform. According to the literature [15], there are negligible differences between these two methods, having the Hilbert Transform a slight advantage. In terms of hardware implementation, the Hilbert Transform is implementable with digital hardware, thus more efficient. The resultant Analytical Signal is defined as:

$$y(t) = x(t) + j\hat{x}(t) \quad (1)$$

Where $\hat{x}(t)$ is the Hilbert Transform of $x(t)$, while the Hilbert transform of $x(t)$ is the convolution of $x(t)$ by $1/\pi$ and can be expressed as:

$$\hat{x}(t) = \frac{1}{\pi} P.V. \int_{-\infty}^{+\infty} x(\tau) \frac{1}{t - \tau} d\tau \quad (2)$$

Here P.V. indicates that the integral is computed in the sense of the Cauchy Principal Value [17]. The phase for each channel is then computed by the Equation (3), where $\text{atan}()$ is defined between $[-\pi/2, \pi/2]$:

$$\theta(t) = \text{atan}\left(\frac{\hat{x}(t)}{x(t)}\right) \quad (3)$$

The computed phases from both active and reference channels are applied to the seizure prediction algorithms. A representative result of computed phases of a seizure episode of a patient is shown in Figure 2 (after unwrapping and detrending of phases).

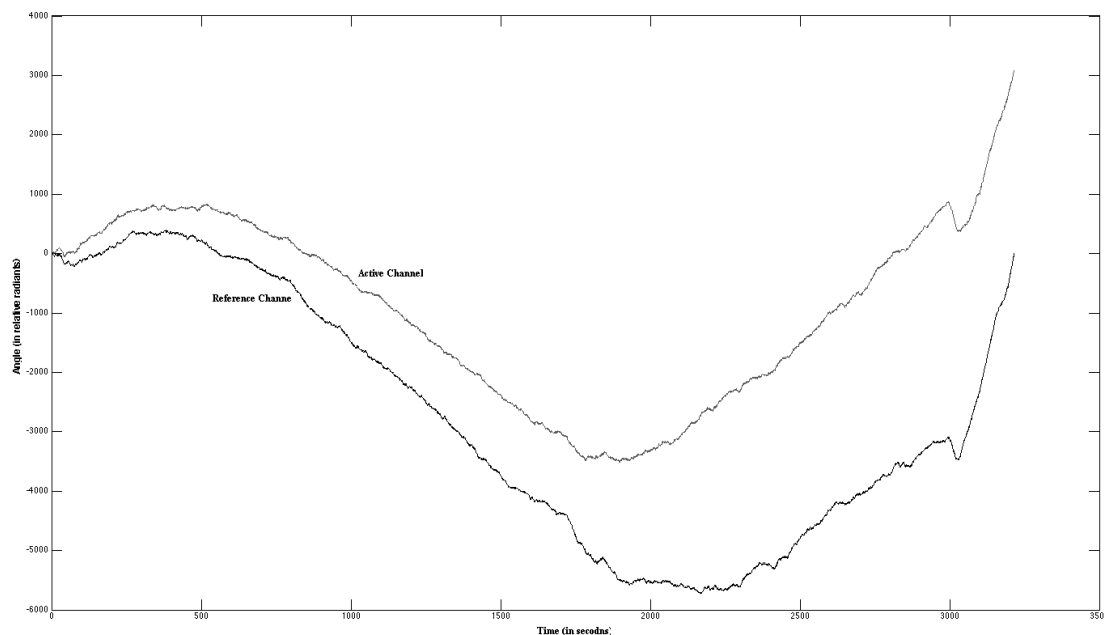


Figure 2. The computed phases from two raw EEG datasets for a patient (ID: chb01, Record: 03). The two channels (active and reference) are channels 21 and 20, which corresponds to FT9-FT1 and T7-FT9, respectively.

2.3 Seizure Prediction

Once the phases for each channel are computed, the next step is to apply the seizure prediction algorithm. In this study, we consider two prediction methods: one is based on Phase-Locking Statistics, presented first in 1999 [9], while the other is Phase Difference method that we propose herein that is hardware-efficient.

2.3.1 Phase-Locking Statistics

The Phase-Locking Statistics is also denoted as Phase-Locking Value (PLV). Le Van Quyen *et al.* [15] used a complex Gabor wavelet to extract the phase information, instead of the Hilbert transform, which provides similar results to the Gabor Wavelet as mentioned before [9]. PLS determines latencies at which the phase differences between two signals are phase-locked or varies slightly across trials [15]. The variance of the phase difference on the unit circle in the complex plane quantifies the degree of phase-locking [17]. When the two phases are independent, the value of PLS becomes 0, while if there is a constant phase-lag between the signals, then the value of PLS is 1. Mathematically, PLS can be defined as follows:

$$PLS = \frac{1}{n} \left\| \sum_{t=1}^n e^{j[\theta_a(t) - \theta_r(t)]} \right\| \quad (4)$$

Here n is the window size, $\theta_a(t)$ is the angle of signals from the active channel, $\theta_r(t)$ is the angle of signals from the reference channel. In this study, the PLS is computed for every new data input (i.e. every 3.9 ms). The PLS is computed by means of an exhaustive overlapping sliding-window technique, where the window size is 256 which corresponds to 1 second of data. The seizure prediction is determined from the spike beyond a threshold level (highest value before seizure) before the seizure, which is calculated at the end of the time series.

2.3.2 Phase Difference

The proposed hardware efficient seizure prediction method presented in this paper is based on Phase Difference (PD). In consistent with PLS, PD is also calculated for every new input data (i.e. every 3.9 ms) from the mean of the phase-differences using an exhaustive overlapping sliding-window of size 256 (equivalent to 1 second of data). The key advantage of PD over PLS is minimized complexity, given that PLS uses a complex exponential, a non-trivial hardware implementation, whereas PD uses difference function that can maintain the capability of accurately predicting seizure episodes. Mathematically, the Phase Difference is defined by:

$$PD = \frac{1}{n} \sum_{t=1}^n |\theta_a(t) - \theta_r(t)| \quad (5)$$

In order to demonstrate that PLS and PD achieves the same performance, PD needs to produce the same output function shape as PLS. For this purpose, we perform the following mathematical transform, which is computing the shifted complement of the PD analytics:

$$PD^c = \max(PD + |\min(PD)|) - (PD + |\min(PD)|) \quad (6)$$

For the final implementation of the system, there is no need to use Equation (6), since with Equation (5) there is enough information to compute the seizure prediction; instead of detecting the maximum peak one needs to identify the minimum.

3. RESULTS

3.1 Validity of PD as an approximation of PLS

In Figure 3, the representative analytics for both of the prediction algorithm of patient 1 (ID: Chb01, Record: 03) are shown. On the left side, the results for both PD^c (top) and PLS (bottom) analytics are shown where the signal was pre-processed with the FIR filter. On the right side, the results for both PD^c (top) and PLS (bottom) analytics are shown using the IIR filter. It can be noted that the spikes that mark the prediction, marked by arrows, for both PD^c and PLS are located at the same time instant, but have a different magnitude. This repeatedly occurred for all of the seizure dataset. The advantage of the PD method is its algorithmic simplicity which yields to a 2.35 times speed-up in a MATLAB implementation since the computational complexity of the algorithm has been reduced.

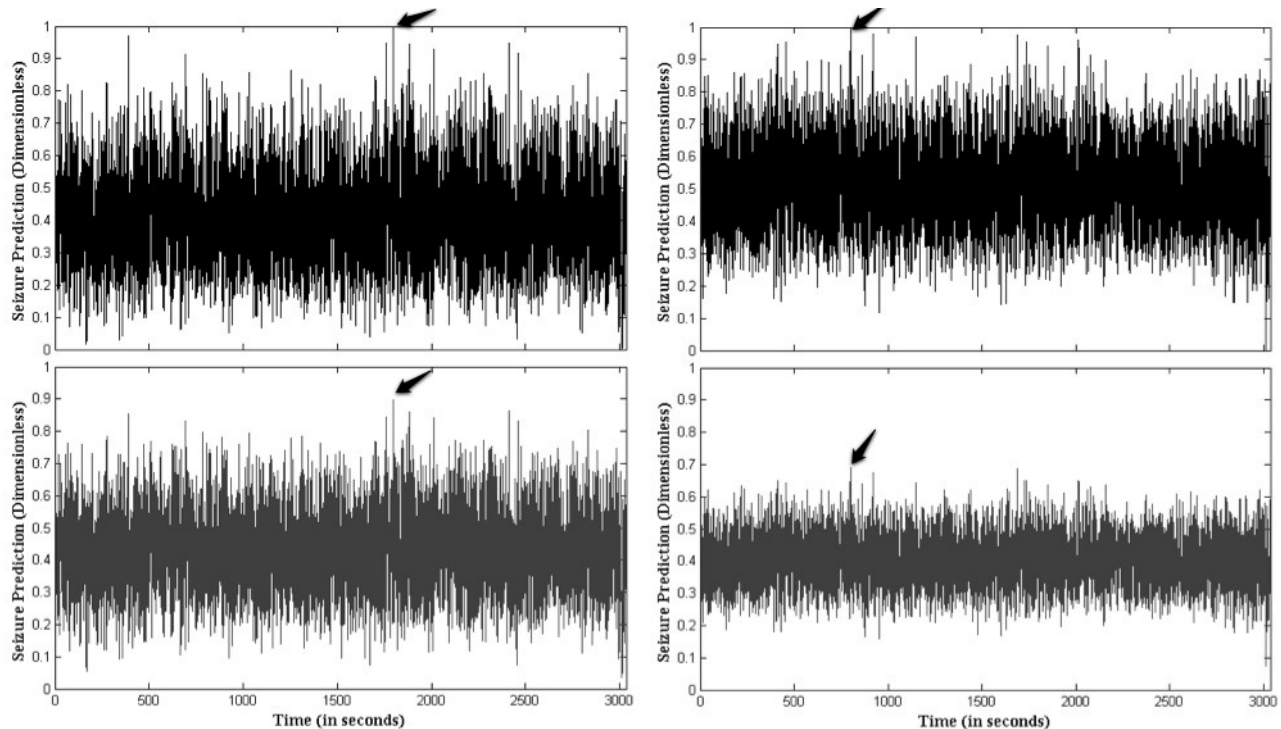


Figure 3. Computed analytics from seizure data for a patient (ID: Chb01, Record: 03). On the left, PD^c (top) and PLS (bottom) analytics using the FIR filter. On the right, PD^c (top) and PLS (bottom) analytics using IIR filter. Arrows mark predicted seizure episodes.

3.2 Peak values for the Seizure Prediction

As it has been demonstrated that for both FIR and IIR filters, both PD^c and PLS produce the peaks at the same time instants, the further analysis of the seizure recordings for the patients (ID: Chb01 to Chb10) is computed using PD^c with the IIR filter, since the corresponding hardware implementation will yield a smaller footprint, reduced complexity, reduction in computational latency, and decreased power consumption.

Next, we analyze if there is a prediction of the seizures for all patients when there is a seizure episode, and that the value is high and distinct enough so it can be consider a prediction marker. In Table 2 the amplitude of the seizure prediction for each recording of every patient is tabulated. The seizure predictor is chosen by calculating the PD^c function for the complete recording, and by selecting the peak spike that occurs prior to the seizure event.

Table 2. Amplitude of the seizure predictor analytics calculated by applying the PD^c on the EEG dataset pre-processed with the FIR filter

Seizure Occurrences	Patient 1	Patient 2	Patient 3	Patient 4	Patient 5	Patient 6	Patient 7	Patient 8	Patient 9	Patient 10
1	0.987	0.8535	0.8343	0.9755	0.9798	0.9254	0.969	0.9865	0.9895	0.9716
2	0.9153	0.9912	0.9641	0.9751	0.8636	0.9653	0.9795	0.9624	0.9628	0.977
3	0.9249	0.9865	0.9649	0.9606	0.901	0.9803	0.9893	0.9675	0.9541	0.9791
4	0.9721		0.9744		0.9905	0.7636		0.9905		0.9341
5	0.9687		0.9724		0.9783	0.9662		0.9601		0.9794
6	0.9853		0.9556			0.9522				
7	0.9679		0.9798			0.9746				
8						0.9749				
9						0.9664				
10						0.9725				

The average of these seizure prediction analytics for the patients is plotted in Figure 4, along with the standard deviation (box) and error range (error bar). For most patients, the values range close to unity with little variations among them and low standard deviations. Conveniently, threshold values can be attributed to each patient, but will differ among patients.

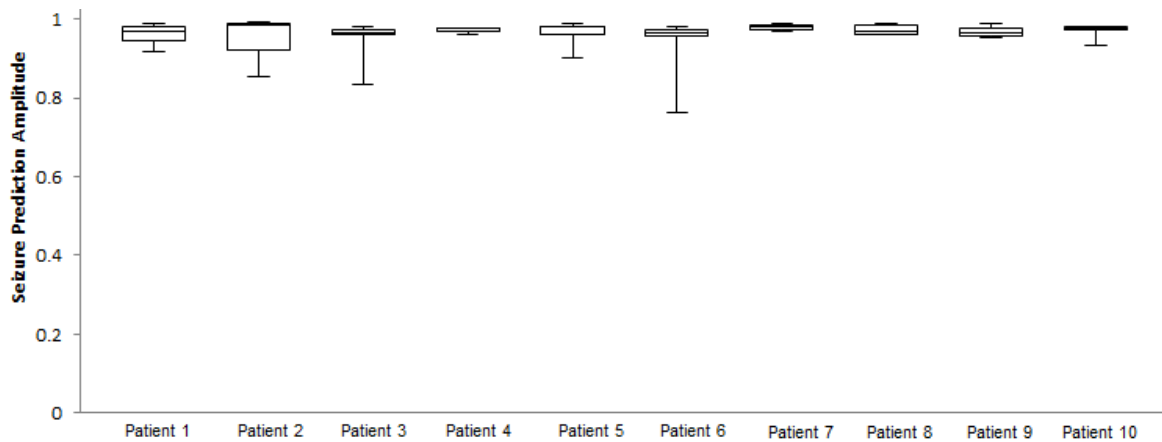


Figure 4. Statistical analysis of amplitude of the seizure predictors (average shown as midline, standard deviation shown as box, and error range shown as error bar).

3.3 Prediction latency

After the seizure predictor operation is validated, we can compute the prediction latency, the time that the seizure prediction is made and the time that the actual seizure episode starts (which is marked by an epileptologist), detected by means of a linear based classifier. Table III shows the obtained prediction latency for every seizure occurrence of every patient within the dataset.

Table III. Prediction latency in minutes for each seizure episode for the patients calculated by applying the PD^c on the EEG dataset pre-processed with the FIR filter

Seizure Occurrences	Patient 1	Patient 2	Patient 3	Patient 4	Patient 5	Patient 6	Patient 7	Patient 8	Patient 9	Patient 10
1	19.97	0.95	2.12	47.97	4.4	7.1	62.87	19.58	62.38	6.63
2	5.93	30.05	4.02	58.47	6.55	8.85	18.75	38.63	21.38	28.7
3	6.77	44	1.7	17.85	10.12	72.93	188.85	25.52	74.52	14.67
4	8.83		11.25		13.43	4.87		25.55		49.63
5	8.78		10.38		5.65	42.73		28.45		8.92
6	0.88		26.7			61.88				
7	1.57		14.48			44.78				
8						5.85				
9						51.38				
10						14.73				

In Figure 5, the average latency is plotted along with the standard deviation (box) and error range (error bar). As it can be noted the values vary to some extent among the patients, evident from high inter-patient standard deviations. For some patients, the large standard deviation is observed. However, in all cases, there exists a seizure prediction marker, ranging between 188 minutes to 57 seconds before the seizure episode starts. This latency is sufficient enough to design a close-loop system that would apply the countermeasures (such as just-in-time VNS stimulation) so that the seizure episode can be subdued or even eliminated.

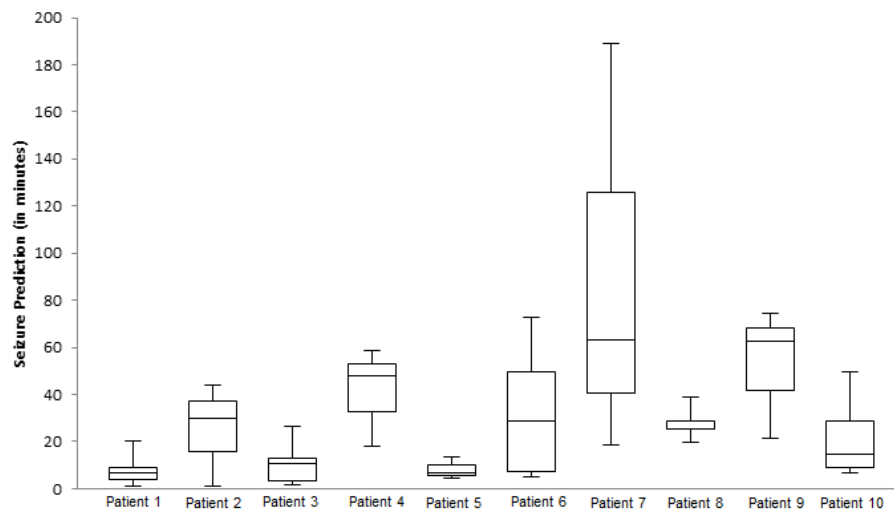


Figure 5. Statistical analysis of the seizure prediction latency (average shown as midline, standard deviation shown as box, and error range shown as error bar).

3.4 Performance Evaluation

For this evaluation, a true positive is considered a peak value of the Phase Difference greater than 0.92 (threshold). A total of 51 seizure events have been analyzed. The sensitivity value calculated is 88.2%, with 45 true positives and 6 false negatives, and the average correct rate of 88.2%, with 45 correctly classified instances. Here, the sensitivity and the correct rate are calculated based on standard expressions provided elsewhere [18]. In this case, a generalized threshold is applied on all patients, which provides a lower bound of performance. Improvement will occur with patient specific thresholds – the most appropriate approach.

4. DISCUSSION

We note that in Section 3.2 for patients 2, 3 and 6, there are a few seizure markers that show a lower peak values. Specifically, statistics of patient 6 had large discrepancy. We hypothesize that this is attributed to the location of the seizure event in the file. These three patients have the seizure events within the first 500 seconds of the file, which might be due to a missing marker before that (in previous unrecorded or recorded data depending on the patient). Regarding the variations in the results presented in Section 3.3, we note that patient 7 statistical results have very large range of prediction latency compared to any other patient. This needs further investigation with new dataset that would reproduce similar effect.

For this study, a window size of 256, equivalent to 1 second of data, is used. Further studies need to be conducted with a range of window sizes and then analyzed to see if they allow the seizure prediction markers to differentiate from non-seizure markers. We speculate that there will be an optimal window size that will show maximum difference between seizure and non-seizure markers.

Another aspect that could be explored is the amount of overlap while sliding windows. The minimum sliding is 1 data, which is most exhaustive and used in this study, while the maximum is equal to the window size (no overlapping). An optimal solution should exist, when trading off the computational complexity (number of analytics per channel) with hardware efficiency (area, power consumption), with the overlap of the window which is not exhaustive.

5. CONCLUSIONS

In this paper, PLS along with hardware efficient PD methods have been studied. PD method has shown the same functional performance as PLS, yielding the same seizure prediction markers. The advantage of the PD method over PLS is algorithmic simplicity yielding up to 2.35 times faster operation in MATLAB implementation due to the reduced computational complexity of the algorithm. With a threshold value of 0.92, 88.2% sensitivity is achieved for a total of 51 seizure episodes, which will improve with personalized threshold settings. Seizure prediction latency was between 188 minutes to 51 seconds.

Our future research direction would include exploring the effects of the window size and the overlap in between the windows in the computation of the Phase Difference to determine the optimal values. We will also investigate the hardware implementation of the PD method.

ACKNOWLEDGEMENTS

The authors would like to thank Rafael Morais, undergraduate student, Universidade Federal do Paraná, Brazil, and Zachary Tate, undergraduate student, Electrical and Computer Engineering Department, The University of Memphis, USA, for their help provided throughout this work.

REFERENCES

- [1] Raghunathan, S *et al.*, "The design and hardware implementation of a low-power real-time seizure detection algorithm", J. Neural Eng., Vol. 6 (5), (2009) .
- [2] Skarpaas, T.L. *et al.*, "Intracranial Stimulation Therapy for Epilepsy", Neurotherapeutics, Vol.6 (2), 238-43 (2009)
- [3] Chen.T *et al.*, "A Hardware Implementation of Real-Time Epileptic Seizure Detector on FPGA", BioCAS, 25 - 28 (2011).
- [4] George, M.S. *et al.*, "Vagus Nerve Stimulation: A New Tool for Brain Research and Therapy", Biol Psychiatry, Vol. 47 (4), 287-95 (2000).
- [5] Blumer D, Rice S, Adamolekun B., "Electroconvulsive treatment for nonepileptic seizure disorders", Epilepsy Behav., Vol. 15 (3), 382-387 (2009).

- [6] Lian, J. *et al.*, "Local Suppression of Epileptiform Activity by Electrical Stimulation in Rat Hippocampus In Vitro", *J Physiol.*, Vol. 547 (2), 427–434 (2003).
- [7] Frei, M.G., Osorio, I., "Left Vagus Nerve Stimulation with the Neurocybernetic Prosthesis Has Complex Effects on Heart Rate and on Its Variability in Humans", *Epilepsia*, Vol. 42 (8), 1007–1016 (2001).
- [8] Theodore, W.L. and Fisher, R., "Brain stimulation for epilepsy", *The Lancet Neurol.*, Vol. 3 (2), 111-118 (2004).
- [9] Jean-Philippe Lachaux *et al.*, "Measuring Synchrony in Brain Signals", *Hum Brain Mapp.*, Vol. 8 (4), 194-208 (1999).
- [10] Le Van Quyen M, Martinerie J, Navarro V, Baulac M, Varela FJ, "Characterizing neurodynamic changes before seizures". *J Clin Neurophysiol.*, Vol. 18 (3), 191-208 (2001).
- [11] Khan, Y.U. *et al.*, "Automatic Detection of Seizure Onset in Pediatric EEG", *IJESA*, Vol. 2 (3), (2012).
- [12] Shueb, A., "Application of Machine Learning to Epileptic Seizure Onset Detection and Treatment". PhD Thesis, Massachusetts Institute of Technology, 2009.
- [13] Goldberger AL, Amaral LAN, Glass L, Hausdorff JM, Ivanov PCh, Mark RG, Mietus JE, Moody GB, Peng C-K, Stanley HE. PhysioBank, PhysioToolkit, and PhysioNet: Components of a New Research Resource for Complex Physiologic Signals. *Circulation* 101(23):e215-e220 "Circulation Electronic Pages; <http://circ.ahajournals.org/cgi/content/full/101/23/e215>; 2000 (June 13).
- [14] Myers, M.H. and Kozma, R., "Seizure Prediction through Dynamic Synchronization Measures of Neural Populations", *Proceedings of IJCNN*, 3500-3506 (2009).
- [15] Le Van Quyen, M., *et al.*, "Comparison of Hilbert Transform and wavelet methods for the analysis of neuronal synchrony", *J Neurosci Methods.*, Vol. 111 (2), 83-98 (2001).
- [16] Freeman *et al.*, "Application of Hilbert transform to scalp EEG containing EMG", *Hum Brain Mapp.*, Vol. 19, 248-272 (2003).
- [17] Navarro, V. *et al.*, "Loss of Synchrony in an animal model of partial status epilepticus", *Neuroscience.*, Vol. 148 (1), 304-13 (2007).
- [18] Pang, C.C *et al.*, "A Comparison of Algorithms for Detection of Spikes in the Electroencephalogram", *IEEE Trans Biomed Eng.*, Vol. 50 (4), 521-526 (2003).